Centralized Disturbance Detection in Smart Microgrids With Noisy and Intermittent Synchrophasor Data

Seyedi, Younes; Karimi, Houshang; Guerrero, Josep M.

Published in:
I E E E Transactions on Smart Grid

DOI (link to publication from Publisher):
10.1109/TSG.2016.2539947

Publication date:
2017

Document Version
Accepted author manuscript, peer reviewed version

Centralized Disturbance Detection in Smart Microgrids With Noisy and Intermittent Synchrophasor Data

Younes Seyedi, Houshang Karimi, *Senior Member, IEEE* and Josep M. Guerrero, *Fellow, IEEE*

***Abstract*—Microgrids are prone to network-wide disturbances such as voltage and frequency deviations. Detection of disturbances by a microgrid central controller (MGCC) is therefore necessary for improving the network operation. Motivated by this application, this paper presents a new structure for the centralized detection of disturbances with noisy synchrophasor data and packet delay/dropouts. We build the proposed structure starting from the analysis of noise-delay tradeoff in synchrophasor networks, and developing a new phasor data concentrator (PDC) for compensation of data losses. The statistical performance metrics of the disturbance detector are numerically evaluated in the case of islanding detection, corroborating that the centralized detector counteracts the measurement noise and lowers the detection time. Numerical results show that the proposed structure significantly mitigates the probability of false detection. Moreover, it can achieve the lower bound of average detection time in a wide range of packet drop rates. This study is useful to network designers who need to employ data acquisition systems for reliable and robust microgrid control applications.**

***Index Terms*—Distributed generation, Disturbance detection, Microgrid control, Synchrophasor network, Smart grid**

I. Introduction

Modern power grids are shifting towards wide area networks with multitude of interconnected microgrids. A microgrid itself is a localized network of distributed generation (DG) systems, dispersed loads, and smart devices capable of bi-directional exchange of power [1]. Such networks give rise to new challenges regarding control, stability, autonomous operation, and power quality assurance [2].

The hierarchical control structure is deemed to be an effective paradigm for large-scale power systems with high penetration of DG systems and microgrids [2]. At the first layer of hierarchical structure, local controllers are responsible for decentralized control of current/voltage or frequency [3]. To this aim, each operating DG system requires high-rate information about the instantaneous voltage and current at its local point of common coupling (PCC) [4], [5]. At the second layer of hierarchical structure, the microgrid central controller (MGCC) is responsible for networked control of microgrid. The main advantage of networked control by the MGCC is improved robustness against disturbances which are not settled by the first layer of control structure. The MGCC receives the data from spatially distributed PCCs. This implies that the MGCC requires synchronized (time-aligned) data which can be obtained by means of phasor measurement units (PMUs) [6]- [9].

In general, the term disturbance refers to any deviation in a power system parameter which may result in stability, power quality or safety issues, and needs to be accommodated for by the controllers in different levels. Transition of microgrid from grid-connected mode to islanded mode is known to be an important source of network-wide disturbance [10]- [13]. For example, in order to ensure the proper operation of microgrid, the MGCC can coordinate all DG systems upon islanding detection and confirmation. The command received by a DG unit can be a change in local controller's parameter, disconnection of DG, or triggering a grid-forming local controller [12]. Another case of network-wide disturbance arises when the microgrid is operating in the islanded mode. In a droop-controlled islanded microgrid, the steady state values of frequency and voltage amplitude deviate after change of load or generation [21]. Under such circumstances, the centralized disturbance detector triggers the restoration process whenever the generated/demanded power changes.

Applications of synchrophasor data for detection, monitoring and control purposes in power systems are addressed in several works [14]- [20]. The previous works attempt to detect network states or transitions by assuming that the phasor data are available from a single measurement unit without any loss of information. However, in realistic microgrids, the time domain measurements are vulnerable to both noise and random losses. It is also known that fast detection of disturbances is of crucial importance in time-critical control applications. Another shortcoming of existing works is that they do not address evaluation of the detection time. To be more precise, they assume that any deviations in the power system parameters are immediately detectable by the controller, i.e., a detection time equal to zero which is far from realistic conditions. It turns out that the centralized disturbance detection based on synchrophasor data subjected to noise, delay, and packet dropout has not been fully investigated. In fact, monitoring of microgrid based on dispersed measurement units invokes a rigorous analysis of reliability and robustness of the detection process which is one of the main contributions of this paper.

The MGCC uses communication systems to supervise and manage DG units in terms of power sharing and compensation of unsettled deviations [1]. Therefore, centralized detection of disturbances can be implemented at a very low cost as

Y. Seyedi and H. Karimi are with the Department of Electrical Engineering, Polytechnique Montreal, Montreal, QC, H3T 1J4, Canada. J. M. Guerrero is with the Department of Energy Technology, Aalborg University, 9220 Aalborg East, Denmark (emails: s.y.seyedi@ieee.org, houshang.karimi@polymtl.ca, joz@et.aau.dk)

long as the microgrid conforms to a hierarchical control structure. On the other hand, communication systems may cause impairments in terms of delay and packet dropouts. Hence, a robust disturbance detection structure is necessary to cope with such impairments at the higher levels of hierarchical control.

In this paper, a new structure for centralized detection of disturbances with noisy and intermittent synchrophasor data is proposed. To achieve a robust and reliable disturbance detection, a new phasor data concentrator (PDC) is developed that efficiently compensates data losses in communications between PMUs and the MGCC. Moreover, the proposed structure mitigates the data noise, reduces the probability of false detection and lowers the average detection time. To evaluate the statistical performance of the proposed structure, a passive islanding detection scenario for a residential microgrid is simulated. The numerical results show that the proposed structure achieves the lower bound of average detection time in a wide range of packet drop rates. The study presented in this paper can aid the designers of smart microgrids in choosing the proper data acquisition systems for reliable and robust microgrid control applications.

It should be noted that islanding detection is just a case study for numerical evaluation of the performance of the proposed disturbance detection structure. Secondary and tertiary control applications in smart microgrids require real-time detection of deviations in the power system parameters. Apart from islanding detection, advanced control functionalities of the MGCC which deal with restoration of frequency and voltage amplitude can be accomplished based on the centralized detection of deviations in frequency and voltage amplitude.

II. Data Acquisition in Smart Microgrids

A. Synchronized Parameter Estimation

Suppose that power system parameters need to be measured at the local PCCs of L DG units. The structure of centralized disturbance detection including L PMUs is depicted in Fig. 1. The PMUs provide the measurement time tags, estimates of phasor magnitude, phase angle, frequency, and rate of change of frequency (ROCOF) of voltage/current signals. The voltage/current signals of the l^{th} PCC ($1 \leq l \leq L$) are corrupted by input noise, $\varepsilon_l(t)$, before they enter the PMU. The functional block diagram of a typical PMU for synchronized parameter estimation is shown in Fig. 1. Let $v_l(t)$ denote the sinusoidal waveform of the voltage of the l^{th} PCC at the time t:

$$v_l(t) = A_l(t)\sin\big(2\pi f_0 t + \theta_l(t)\big), \quad 1 \leq l \leq L, \qquad (1)$$

where f_0 is the nominal frequency of the power system. This waveform can be represented by a phasor as

$$V_l(t) = \frac{A_l(t)}{\sqrt{2}} e^{j\theta_l(t)}. \qquad (2)$$

The input signal is first filtered to attenuate frequency components which are above the Nyquist frequency of the internal sampling process. An analog-to-digital (A/D) converter takes samples of the filtered signal at the rate F_s samples/sec. At the time instant $t = i/F_s$, $(i = 0, 1, 2, ...)$ the parameter estimator calculates the phasor magnitude $A_{l,i}$ and the phase angle $\theta_{l,i}$ which lies in the interval $[-\pi, \pi]$. The parameter estimator can be realized using either of fast Fourier transform (FFT), enhanced phase locked loop (EPLL) [22] or unified three-phase signal processor (UTSP) [24]. The UTSP is basically an enhanced three-phase PLL which has an integral structure and estimates phasors of voltage/current signals along with frequency and ROCOF. The UTSP parameters are real positive gains denoted by μ_i, $i = 1, 2, ..., 7$, which can be tuned to yield the desired speed of estimation. A detailed design procedure of gains μ_i are discussed in [24]. One advantage of the UTSP is that it can estimate the phasors, frequency and ROCOF with good immunity to noise and fast response time [24], [25].

Due to presence of harmonics and noise in the input signals, the estimated phasors are noisy versions of the true phasors. Let $n_{l,A,i}$ and $n_{l,\theta,i}$ denote the additive noise in the magnitude and phase angle, respectively. It follows that

$$A_{l,i} = A_l(\frac{i}{F_s}) + n_{l,A,i}, \qquad \theta_{l,i} = \theta_l(\frac{i}{F_s}) + n_{l,\theta,i}. \qquad (3)$$

The parameter estimator must also provide the samples of instantaneous frequency $f_{l,i}$ and the instantaneous ROCOF $\delta_{l,i}$. It is concluded that

$$f_l(t) = f_0 + \frac{1}{2\pi}\frac{d}{dt}\theta_l(t), \qquad \delta_l(t) = \frac{d}{dt}f_l(t), \qquad (4)$$

and

$$f_{l,i} = f_l(\frac{i}{F_s}) + n_{l,f,i}, \qquad \delta_{l,i} = \delta_l(\frac{i}{F_s}) + n_{l,\delta,i}, \qquad (5)$$

where $n_{l,f,i}$ and $n_{l,\delta,i}$ denote the additive noise in frequency and ROCOF, respectively.

The IEEE standard C37.118.1-2011 [6] defines a data frame as a set of phasor, frequency, and ROCOF samples that correspond to the same measurement time tag. To construct a data frame, let $\mathbf{s}_l(t) = [A_l(t)\ \theta_l(t)\ f_l(t)\ \delta_l(t)]^T$ and $\mathbf{n}_{l,i} = [n_{l,A,i}\, n_{l,\theta,i}\, n_{l,f,i}\, n_{l,\delta,i}]^T$ denote the vector of true parameters and the data noise, respectively. The output of the parameter estimator is thus the following data frame:

$$\mathbf{u}_{l,i} = [A_{l,i}\ \theta_{l,i}\ f_{l,i}\ \delta_{l,i}]^T = \mathbf{s}_l\big(\frac{i}{F_s}\big) + \mathbf{n}_{l,i}. \qquad (6)$$

Our comprehensive simulations based on the UTSP and Kolmogorov-Smirnov test verify that the noise in the data frames fits well to the Gaussian distribution, hence, $\mathbf{n}_{l,i}$ are assumed to be Gaussian random vectors.

A windowing operation can be applied on the output of the parameter estimator followed by a decimator which produces a data stream suitable for transmission to the MGCC. The downsampling is required before transmission of data frames since the internal sampling rate of three-phase signals is much higher than the reporting rate. It is worth mentioning that, windowing (as viewed as low-pass filtering) offers several advantages: it can mitigate the adverse input noise, attenuate abrupt transients due to sudden load changes, and remove the aliasing effect in the downsampling process [6].

Suppose that the data frames are filtered by a finite-duration

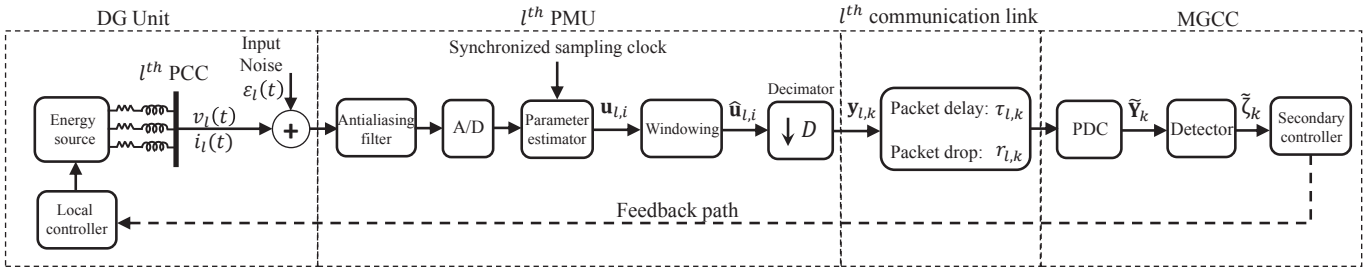

Fig. 1: Centralized disturbance detection with noisy and intermittent synchrophasor data

window of length $N+1$, i.e., $N+1$ shows the number of consecutive data vectors that are simultaneously used in the windowing process. For even number N, windowing results in the following vector relationship:

$$\hat{\mathbf{u}}_{l,i} = \frac{1}{W} \sum_{m=-N/2}^{N/2} w_m \ \mathbf{u}_{l,i+m} \tag{7}$$

where $W \triangleq \sum_{m=-N/2}^{N/2} w_m$, and w_m are the real coefficients of the window. Note that the measurement time tag must be computed according to the center of the window with compensation for any preceding delays. Once filtered samples are decimated, they can be reported to the MGCC at the rate F_t frames per second (fps). Now, let D represent the integer decimation factor, i.e., $D = F_s/F_t$, the k^{th} data frame which is transmitted from the l^{th} PMU is the vector

$$\mathbf{y}_{l,k} = \hat{\mathbf{u}}_{l,kD}, \quad k = 0, 1, 2, ..., \ 1 \le l \le L. \tag{8}$$

B. Noise-Delay Tradeoff in Data Acquisition

According to (6) and (7), harmonics distortion and input noise result in estimation errors which are accounted for by the data noise vectors $\mathbf{n}_{l,i}$. In general, the statistics of $\varepsilon_l(t)$ have a direct impact on the statistics of the data noise vector. Due to structural complexity of the estimator [25], explicit analysis of the behavior of the data noise is not mathematically tractable. The parameter estimator includes several feedback loops which are strongly coupled. Therefore, the elements of the data noise vector become correlated to each other. Moreover, the noise samples in each parameter are correlated in time. It is thus crucial to obtain a valid model for the effective noise in data frames. To this aim, suppose that $\varepsilon_l(t)$ is a zero-mean Gaussian noise and its statistics are fixed. The additive noise that enters the l^{th} parameter estimator is therefore a white Gaussian noise with zero mean and fixed variance σ_l^2.

Let $\hat{\mathbf{n}}_{l,k}$ represent the effective (after windowing) data noise vector in the k^{th} data frame. It follows from (6)-(8) that

$$\hat{\mathbf{n}}_{l,k} = \frac{1}{W} \bar{\mathbf{n}}_{l,kD} \mathbf{w}, \tag{9}$$

where $\bar{\mathbf{n}}_{l,kD} = [\mathbf{n}_{l,kD-N/2} \cdots \mathbf{n}_{l,kD} \cdots \mathbf{n}_{l,kD+N/2}]$, and $\mathbf{w} = [w_{-N/2} \cdots w_0 \cdots w_{N/2}]^T$ is the vector of window coefficients. The correlation matrix of the effective noise is therefore given by $\mathbf{R}_l = \mathbb{E}\{\hat{\mathbf{n}}_{l,k} \hat{\mathbf{n}}_{l,k}^T\} = \frac{1}{W^2} \mathbb{E}\{\bar{\mathbf{n}}_{l,kD} \mathbf{w}\mathbf{w}^T \bar{\mathbf{n}}_{l,kD}^T\}$. Based on the premise that the input noise is stationary within the estimation interval, the correlation matrix $\mathbf{R}_l$ is independent of time. In what follows, the variable x represents a parameter belonging to the set $\mathcal{P} = \{A, \theta, f, \delta\}$. The autocorrelation of the noise in the parameter x is given by $R_{l,x}(i,j) = \mathbb{E}\{n_{l,x,i} n_{l,x,j}\}$.

An important statistical quantity is the variance of the effective noise when the power system is in the steady state, i.e., the input voltage and current signals are not in a disturbed or transient condition. The variance of the effective noise in each parameter can be assessed by:

$$\hat{\sigma}_{l,x}^2 = \frac{1}{W^2} \left[\mathbf{w}^T \mathbf{w} \sigma_{l,x}^2 + \sum_{\substack{i=-N/2 \\ i \neq j}}^{N/2} \sum_{j=-N/2}^{N/2} w_i w_j R_{l,x}(i,j) \right] \tag{10}$$

where $\sigma_{l,x}^2 = \mathbb{E}\{n_{l,x,i}^2\}$ represents the noise variance in parameter x at the l^{th} PMU (without windowing) which depends on the input noise variance σ_l^2, and the type of parameter estimator. Our studies show that for each parameter $x \in \mathcal{P}$ the data noise is correlation q-dependent [27], i.e., there is a positive number q such that

$$R_{l,x}(i,j) = 0, \qquad |i-j| > q, \quad \forall x \in \mathcal{P}.$$

For a given F_s, the values of q can easily be found for the noise process in the parameter of interest.

A basic post-estimation window is the moving average which can be realized by a rectangular window [26]. If a rectangular window with $N \ge q$ is used, then (10) yields

$$\hat{\sigma}_{l,x}^2 = \frac{1}{N+1} \sigma_{l,x}^2 + \frac{1}{(N+1)^2} K_{l,x} \tag{11}$$

where $K_{l,x}$ is a constant given by

$$K_{l,x} = \sum_{\substack{i=-q/2 \\ i \neq j}}^{q/2} \sum_{j=-q/2}^{q/2} R_{l,x}(i,j).$$

Eq. (11) reveals that the variance of the effective noise in the synchrophasor data frames depends on $\sigma_{l,x}^2$, the length of window, and the type of parameter estimator (through the parameter $K_{l,x}$). As a consequence of windowing, a non-trivial delay is imposed on the data frames. The data acquisition delay

is given by

$$\tau_{pmu} = \frac{N}{2F_s} + \tau_p. \tag{12}$$

The first term in (12) indicates the group delay due to windowing and the second term, τ_p, represents the PMU processing time including any pre-estimation delay caused by antialiasing filters. Eq. (11) reveals that under windowing with $N > q$, the variance of the effective noise in each data frame is roughly reduced by a factor $1/N$. On the contrary, data acquisition delay linearly increases with increasing N. This tradeoff between the effective noise variance and the data acquisition delay has an impact on the accuracy and latency of disturbance detection using synchrophasor networks.

III. The Impact of Communication Systems

Centralized disturbance detection and hierarchical microgrid control are dependent on the quality of service provided by communication systems [21]. By employing several PMUs, the parameters of local PCCs can be extracted in a synchronized manner with constant acquisition delay. However, communication systems may introduce impairments [23] and therefore, the actual synchrophasor data as seen by the MGCC become intermittent.

In general, either of transmission control protocol (TCP) or user datagram protocol (UDP) [7] can be used for transmission of data packets. By adopting the TCP, once an erroneous data packet is detected, the receiver requests retransmission of the packet from the corresponding transmitter. On the contrary, by employing the UDP, the erroneous data packet is simply dropped at the receiver. Hence, no further delay is imposed on the subsequent data packets waiting to be transmitted. Erroneous data packets can be detected by means of error detection coding, e.g., cyclic redundancy codes [7]. The inevitable request and reply process in the TCP [29] can cause intolerable delay for time-critical applications such as disturbance detection and protection of microgrid. It can be concluded that the UDP is more efficient for communications between PMUs and the MGCC, whereas the TCP is a good candidate for communications between the MGCC and the local controllers.

If the UDP is employed for transmission of data packets, the l^{th} communication link can be characterized by a packet delay variable, $\tau_{l,k}$, and a binary random variable $r_{l,k}$ (refer to Fig. 1). Note that the characteristics of communication links may vary after one reporting interval. Specifically, $\tau_{l,k}$ indicates the total communication delay incurred by the k^{th} data packet in transmission from the l^{th} PMU. Generally, the value of $\tau_{l,k}$ depends on the packet size, reporting rate, communication channel access time, coding time, etc. If a single communication medium (e.g., a wireless channel) is shared among different PMUs, then the communication delay may be affected by congestion and thus $\tau_{l,k}$ will be a random variable. Further characterization of communication links in terms of packet delay is beyond the scope of this paper.

The random variables $r_{l,k}$ indicate delivery status of data packets. The dropped (erroneous) data packets have $r_{l,k} = 0$ and the delivered (error-free) packets have $r_{l,k} = 1$. The Bernoulli distribution specifies the stochastic model of packet dropouts in communication links:

$$\Pr\{r_{l,k} = 0\} = p_{d,l}, \tag{13}$$

$$\Pr\{r_{l,k} = 1\} = 1 - p_{d,l}, \tag{14}$$

where $p_{d,l}$ is the packet drop probability in the link between the l^{th} PMU and the MGCC. The packet drop probability in the links depends on the quality of service provided by the communication system.

The PDC collects and prepares the distributed synchrophasor data for making decision [30]. However, due to the delay requirements of networked control applications, the PDC cannot wait for an arbitrary long time. Instead, the PDC uses a fixed waiting interval [7] and then sends the k^{th} data set arrived within this interval to the detector. A data set, denoted by $\tilde{\mathbf{Y}}_k$ in Fig. 1, is a $4 \times L$ matrix formed by concatenation of distributed synchrophasor data.

Suppose that all PMUs report their data frames at an integer rate F_t fps, and let the reporting instants be evenly spaced through the time. In a one-second interval, each PMU has to send F_t packets and the transmission of the first packet coincides with the coordinated universal time second rollover [6] which is known by all PMUs and the PDC. The PDC which is synchronized with the PMUs anticipates to receive L data packets from L nodes during each $1/F_t$ seconds time interval. In this fully synchronized regime, the estimation, transmission, and concentration of power system parameters are accomplished in a synchronized manner. Consequently, it is plausible to assume that the PDC wait time is equal to one reporting interval.

IV. Centralized Disturbance Detection

A. The PDC Design

In PDC design for hierarchical control, it is important to account for the loss of synchrophasor data caused by delayed arrival or dropouts of packets. The IEEE standard for synchrophasor data transfer [7] declares that a conventional PDC inserts an invalid data indicator (such as NaN) in place of absent data frames. However, data indicators do not facilitate decision making about the network states, hence, conventional PDC algorithms are not efficient for networked control applications. A more elaborate solution is to utilize the set of received data frames with identical measurement time tags in order to extract some elements of the lost data frames.

Once a data packet from a PMU is dropped or intolerably late, each parameter $x \in \mathcal{P}$ for that DG has to be determined. Let $\mathbf{y}_{l,k} = [y_{l,A,k}\ \ y_{l,\theta,k}\ \ y_{l,f,k}\ \ y_{l,\delta,k}]^T$ and $\tilde{\mathbf{y}}_{l,k} = [\tilde{y}_{l,A,k}\ \tilde{y}_{l,\theta,k}\ \tilde{y}_{l,f,k}\ \tilde{y}_{l,\delta,k}]^T$ denote the vector of measured and PDC output data at the k^{th} time index, respectively. At each time index, the PDC employs the set of received frames to reconstruct the lost data. The procedure of data concentration is explained in Algorithm 1 assuming that the PDC wait time is $1/F_t$ sec. Note that by virtue of time tags provided in the data packets, the values of $r_{l,k}$ and $\tau_{l,k}$ are easily found by the PDC.

Algorithm 1:

- **Initialize:** at $k = 0$
  When the microgrid is operating in the steady state condition, the PDC is initialized by the nominal values of the parameters for each PCC.
- **Interpolate and Concentrate:** for each $k > 0$:
  1) Find the indices of links which have delivered their data packets and construct the set: $\mathcal{L}_k \triangleq \{l; r_{l,k} = 1, \tau_{l,k} \leq 1/F_t\}$.
  2) If $|\mathcal{L}_k| = 0$ go to step 3, otherwise step 4.
  3) Set $\tilde{y}_{l,x,k} = \tilde{y}_{l,x,k-1}, l = 1, 2, ..., L, \forall x \in \mathcal{P}$. Proceed to step 1 with time index $k + 1$.
  4) For $l = 1, 2, ..., L$:
     If $l \in \mathcal{L}_k$, set $\tilde{y}_{l,x,k} = y_{l,x,k}, \forall x \in \mathcal{P}$.
     If $l \notin \mathcal{L}_k$, set $\tilde{y}_{l,A,k} = \tilde{y}_{l,A,k-1}$, $\tilde{y}_{l,\theta,k} = \tilde{y}_{l,\theta,k-1}$ proceed to step 5.
  5) For $x \in \{f, \delta\}$, if $\sigma_{l,x}$ are a priori known at the MGC use (15), otherwise (16)*:

$$\tilde{y}_{l,x,k} = \Big(\sum_{j \in \mathcal{L}_k} 1/\sigma_{j,x}^2 \Big)^{-1} \sum_{j \in \mathcal{L}_k} \frac{y_{j,x,k}}{\sigma_{j,x}^2}, \qquad (15)$$

$$\tilde{y}_{l,x,k} = \frac{1}{|\mathcal{L}_k|} \sum_{j \in \mathcal{L}_k} y_{j,x,k}, \qquad (16)$$

  Proceed to step 1 with time index $k + 1$.

*$|\mathcal{S}|$ shows the cardinality of the set $\mathcal{S}$.

According to Algorithm 1, if a data packet is delivered, then it is immediately used in the corresponding data set. In case of a packet dropout or late arrival, the unknown amplitude and phase angle are replaced by the last received samples from the associated PMU, while the system frequency, and ROCOF are interpolated based on the maximum likelihood value (Eq. (15)) or the arithmetic mean of the available samples (Eq. (16)). In distribution microgrids and under the influence of line impedance, the amplitude and phase angle variations can be different at separate PCCs. Nonetheless, the system frequency, and ROCOF are not dependent on the PCC location and the line impedance. To be more specific, Algorithm 1 is recursive in terms of local parameters but interpolative for the global parameters. It should be noted that an interpolative PDC turns into a recursive one if all communication links fail in delivering data packets.

The advantage of Algorithm 1 for hierarchical control applications is twofold. Under intermittent synchrophasor data, a MGCC which uses an interpolative PDC is faster than the one employing a pure recursive PDC. Moreover, the extracted data by an interpolative PDC possess good immunity to measurement noise and PMU failures due to the inherent averaging. Fig. 2 illustrates an example of spatial interpolation for system frequency where only the link of the fourth DG unit incurs packet dropouts.

B. The Central Disturbance Detector

A disturbance can be observed as deviation in some estimated parameters of the power system. However, the synchrophasor data packets bearing such deviations undergo impairments over time. The central detector is fed by a concentrated dataset as produced by the Algorithm 1. Suppose that the detector is making decision about the state of microgrid at the time instant k. The detector calculates the normalized sum of deviations in the selected parameters as follows:

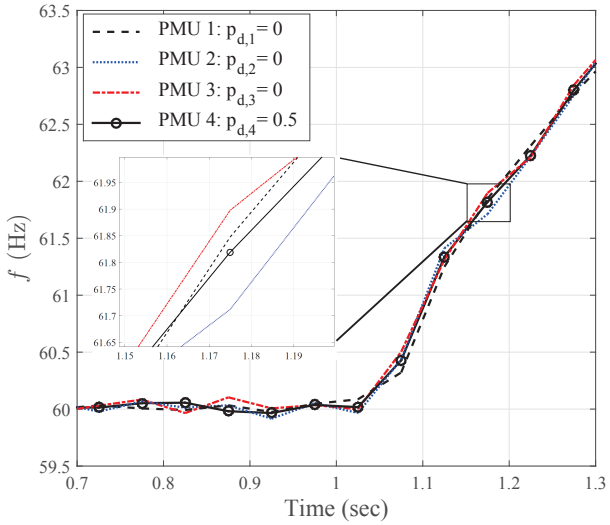

Fig. 2: A snapshot of spatial interpolation under a ramp of system frequency for a microgrid with $L = 4$ PMUs. The circles indicate interpolated samples.

$$\beta_{x,k} = \frac{1}{L} \sum_{l=1}^{L} (\tilde{y}_{l,x,k} - x_0), \qquad (17)$$

where x_0 is the nominal value of the parameter x which is known by the MGCC. Let the binary variables ζ and $\tilde{\zeta}$ represent the true state and the detected state of the microgrid, respectively. If the microgrid is in a disturbed state, then $\zeta = 1$, otherwise $\zeta = 0$. Moreover, $\tilde{\zeta} = 1$ indicates that a disturbance has been detected and the secondary controller must be triggered, while $\tilde{\zeta} = 0$ indicates the normal (non-disturbed) operation of microgrid. The disturbance detection criterion is surpassing a fixed threshold for at least one parameter in $\mathcal{P}$:

$$\tilde{\zeta}_k = \begin{cases} 1, & \text{if } |\beta_{x,k}| > \Gamma_x \\ 0, & \text{otherwise} \end{cases} \qquad (18)$$

where Γ_x denotes the absolute normalized deviation in the parameter x which can be tolerated by the microgrid. A centralized detection method based on (17) and (18) performs very well compared to local detection of voltage or frequency disturbances.

C. Performance of The Central Detector

The performance of the MGCC depends on the accuracy of the central detector in distinguishing the microgrid states. On the other hand, the estimation and transmission of the power system parameters are subjected to data noise, data acquisition delay, packet delay, and random packet dropouts. Therefore,

it is necessary to adopt a statistical approach when evaluating the reliability and performance of the central detector with UDP-based communication links.

At the secondary control layer, it is necessary to take the cumulative detection delay into account. This delay may lead to harmful transients or even instability of the network. To investigate such delays, we define the average detection time, T_d, as the expected value of the interval between the instant of disturbance occurrence and the detection instant by the MGCC. The average detection time is related to the data acquisition delay and the reporting period through the following expression:

$$T_d = \tau_{pmu} + \frac{1}{2F_t} + \tau_e. \tag{19}$$

The second term in (19) measures the average time that the disturbed parameters are transmitted. τ_e shows the expected value of the detection delay which depends on how fast the disturbances are detected after the instant of their data transmission. Dropouts and delayed arrivals of synchrophasor data packets directly affect the value of τ_e. In the fully synchronized regime, the inequality $\tau_e \geq \tau_{pdc} + 1/F_t$ is always maintained and the lower bound for the average detection time is:

$$T_{d,LB} = \tau_{pmu} + \tau_{pdc} + \frac{3}{2F_t}, \tag{20}$$

where τ_{pdc} is the PDC processing time defined in [30]. False detections may result from measurement noise [28], sudden load changes, PMU failures or large timing errors during synchrophasor data acquisition. The probability of false detection is a qualified performance metric under such circumstances:

$$p_{FD} = \Pr\{\tilde{\zeta} = 1 | \zeta = 0\}, \tag{21}$$

where $\Pr\{.|.\}$ represents the conditional probability. In practice, bad PMU measurements can occur and if not properly detected can increase the probability of false detection [31], [32]. This suggests that the disturbance detection structure can be augmented by a bad data identifier which cooperates with the proposed PDC. The resulting structure is an improved disturbance detector which counteracts delays, noises as well as bad data and further mitigates the probability of false detection.

The above metrics are applicable to any secondary and tertiary control applications with noisy and intermittent synchrophasor data. Moreover, they do not impose any constraint on the structure and complexity of the detection algorithm. Generally, the smaller p_{FD}, the more reliable the central detector is. However, imperfect communication systems result in loss of data samples and the robustness of detection process can decrease, i.e., T_d may increase. As soon as a disturbance is detected, the MGCC determines a set of control commands based on the disturbed parameter, the intensity of the disturbance, and the capacities of DG systems. The feedback messages are then sent to the local controllers belonging to the microgrid (refer to Fig. 1).

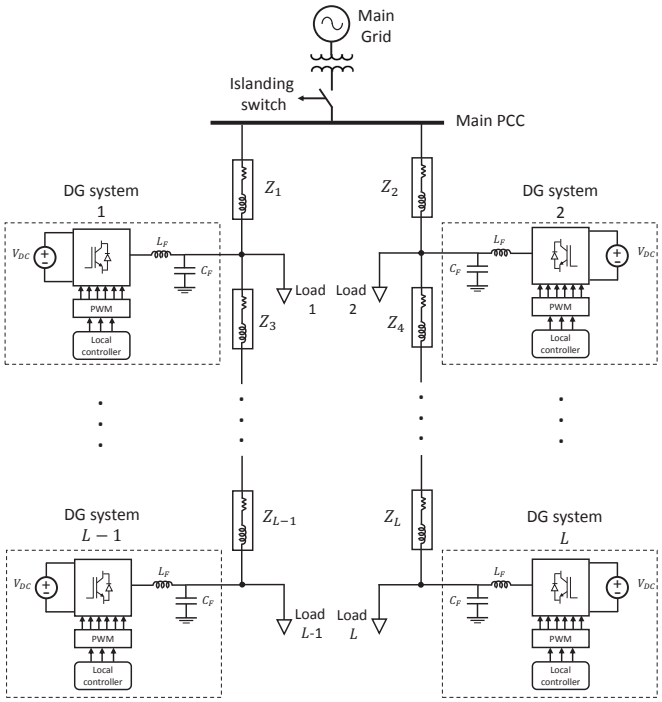

Fig. 3: The single-line schematic of network in a radial microgrid with residential loads.

V. Numerical Results

A. Network Simulation Procedure

As illustrated in Fig. 3, centralized detection is implemented in a residential microgrid including low-voltage photovoltaic energy sources, two feeders, and household loads. It is assumed that the feeders have equal number of sources and loads (i.e., L is even). Each DG system supplies a local consumer and each local PCC has a dedicated PMU. As in the case of most photovoltaic (PV) systems [33], the DG systems are equipped with three-phase voltage-sourced converters (VSCs) which employ local current controllers. In order to make the test scenario a realistic one, the consumers are modeled by independent and random (time-varying) PQ loads. The nominal voltage and system frequency are 380 V and 60 Hz, respectively. The active and reactive powers of loads are uniformly distributed in the interval $[0, 10]$ kW and $[0, 2]$ kVAR, respectively.

The DG systems are responsible for delivering a certain amount of power in the grid-connected mode [13]. The secondary controller matches the generated active power to the average consumed power by setting the reference point of DG systems to $P^* = 5$ kW. All DG units operate under unity power factor, i.e., $Q^* = 0$. Hence the reactive power demanded by the consumers has to be provided by the main grid. In Fig. 3, Z_l represents the model of low-voltage line between different PCCs. The distance between neighboring PCCs is 40 m and the impedance per length is 0.64 Ω/Km. The DC voltage produced by the PV which supplies DG systems is $V_{DC} = 700$ V. The filter inductance and capacitance are $L_F = 15$ mH and $C_F = 10$ μF, respectively. The UTSP is employed for parameter estimation at each PCC with the gains set to $\mu_1 =$

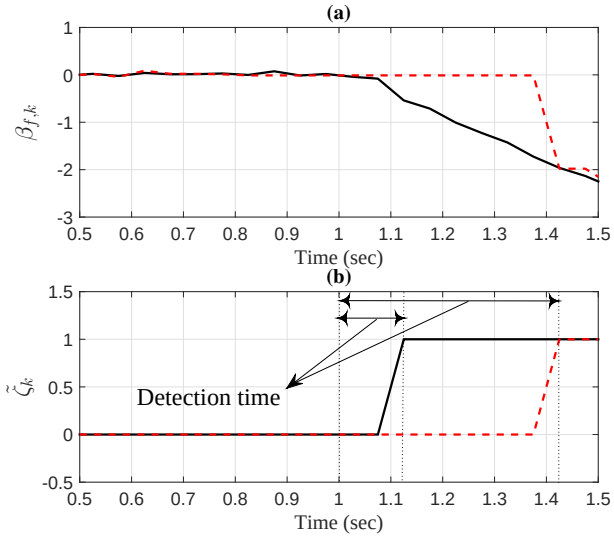

Fig. 4: Cases of fast (solid curves) and slow (dashed curves) detection under packet dropouts. (a): The normalized sum of deviations, (b): The detected state.

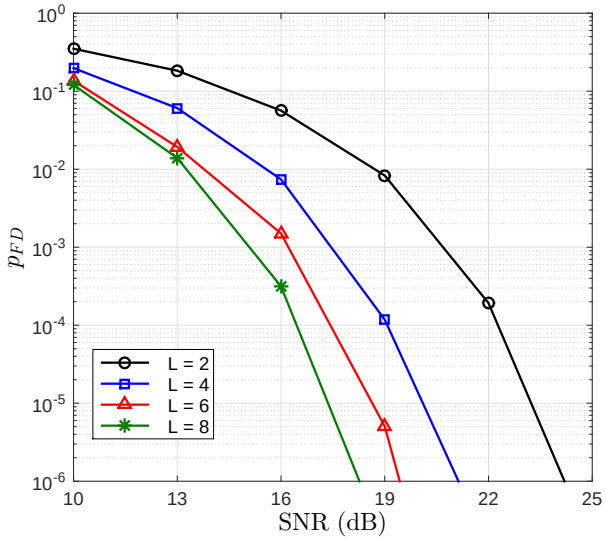

Fig. 5: Probability of false detection in the central detection.

$\mu_2 = \mu_3 = 67, \mu_4 = 20000, \mu_5 = 130, \mu_6 = 433, \mu_7 = 1333$. The gains of UTSP are chosen such that the response time of the estimator is less than one cycle. All PMUs have an internal sampling rate $F_s = 2000$ samples/sec, and unless otherwise stated, the rectangular window with $N = 120$ is employed. The PMU and PDC processing times are $\tau_p = 20$ msec and $\tau_{pdc} = 0$, respectively. The estimated data are transmitted at a rate of one frame every three cycles, i.e., $F_t = 20$ fps.

In this case study, the disturbances to be detected are either system frequency or voltage deviations which occur due to isolation of the microgrid. The desired values of these parameters are $f_0 = 60$ Hz, and $A_0 = 1$ pu. The electrical part of the network is implemented in SimPowerSystems/Simulink and the extracted data frames are further processed by MATLAB which performs communications and detection parts of the hierarchical control process. Extensive Monte Carlo simulations are carried out for performance evaluation of the central detector. The microgrid is islanded at the time instant $t = 1$ sec. For each random realization of PQ loads, the developed algorithms are sequentially invoked and the output of the detector is captured. According to this simulation procedure, a false detection occurs if the value of $\tilde{\zeta}$ changes from 0 to 1 before $t = 1$ sec. In all network simulations, only the measurement noise results in errors and may lead to a false detection. It is assumed that all PMUs work with the same input SNR, and all communication links undergo identical packet drop rates. The parameters $\sigma_{l,x}$ are not a priori known at the MGCC and thus (16) is used for spatial interpolation at the PDC. The packet delays are negligible compared to the reporting interval, i.e., $\tau_{l,k} \ll 1/F_t$. Finally, the time resolution for the detection process at the secondary control layer is 1 msec.

B. Discussion of Results

Time-domain simulation results indicating fast and slow detections with $L = 4$ are shown in Fig. 4. The input SNR is 19 dB and the disturbance threshold is $\Gamma_f = 0.1$ Hz. In the extreme case of slow detection, the arrival of synchrophasor data is such that the PDC cannot update $\beta_{f,k}$ over a long interval. As depicted in Fig. 4 (b), the slow detection time is greater than 24 cycles which may result in a failure of networked control process. In the case of fast detection, however, the detection time is equal to $T_{d,LB}$.

The reliability of the proposed detector in terms of false detections is illustrated in Fig. 5 for different numbers of PMUs. This figure shows the diversity gain provided by the distributed synchrophasor data in the centralized detection methodology. As the number of PMUs increases, the required input SNR at each PMU decreases for a constant p_{FD}. By doubling L, a gain of 3 dB can be procured in the low-SNR region. The simulation results shown in Fig. 6 aim to assess the performance of threshold-based local detection for the test microgrid. In the local method, each DG constantly monitors the absolute value of deviations in locally estimated frequency and amplitude. In Fig. 6, p_{FD} shows the probability that at least one DG indicates an absolute deviation exceeding 0.1 Hz in frequency or 0.1 pu in voltage amplitude. It can be concluded that the local detection methodology performs poor in the low and moderate SNR regions. By comparing the results shown in Figs. 5 and 6, it is evident that the central method is capable of making the high-level control applications more reliable, i.e., p_{FD} is less than 10^{-6} when $\sigma_l^2 \leq -25$ dB. The centralized detection method shows a superior performance over local detection methods in noisy environments. This observation substantiates the necessity of a central detector for efficient hierarchical control of microgrids.

Fig. 7 compares the performances of PDC algorithms in the test microgrid with eight PMUs. The detection time of frequency disturbance with a threshold $\Gamma_f = 0.5$ Hz increases

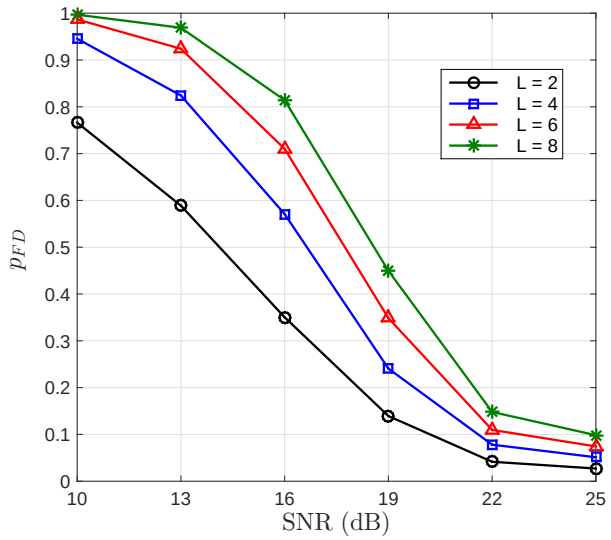

Fig. 6: Probability of false detection in the local detection.

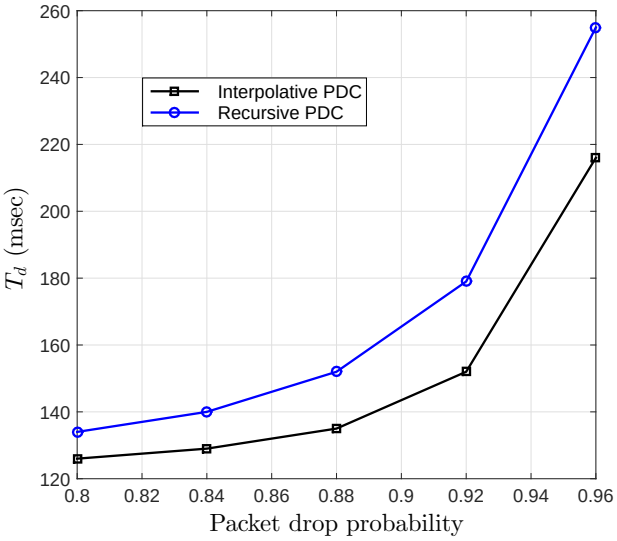

Fig. 7: Performance comparison of interpolative and recursive PDC algorithms, $\Gamma_f = 0.5$ Hz, input SNR = 19 dB.

when the packet drop rate is increased regardless of the PDC algorithm. However, the interpolative PDC leads to a faster detection on average and the control application gains a notable delay margin. This delay margin becomes larger if the packet dropout becomes severe. For packet drop rate of 0.8, the difference between the two detection times is 8 msec and it increases to 39 msec at drop rate of 0.96.

Fig. 8 shows how the detection time will affect the probability of false detection. The noise-delay tradeoff manifests itself in this result. A smaller p_{FD} corresponds to a larger T_d at a fixed input SNR. Moreover, for a given p_{FD}, a greater L results in a smaller T_d. The performance of the detection structure in terms of average detection time is illustrated in Fig. 9. Note that the detection time has a lower bound equal to $T_{d,LB} = 125$ msec. It can be observed that the centralized detector along with the interpolative PDC make the detection process robust against severe packet dropouts. For the microgrid with eight PMUs, T_d is very close to the lower bound expressed in (20). However, it increases gradually if packet dropouts occur at a rate larger than 0.8. As it was anticipated, the highest increment of the average detection time is observed in case of $L = 2$ since the PDC is actually recursive for most of the time.

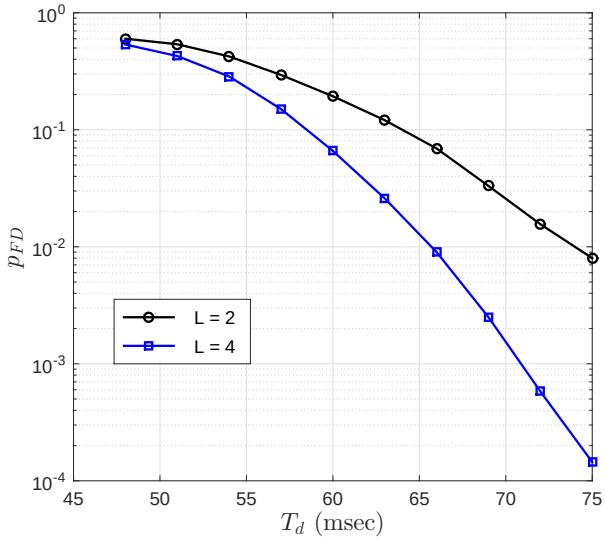

Fig. 8: Probability of false detection vs. average detection time: $\sigma_l^2 = -19$ dB, $p_{d,l} = 10\%$.

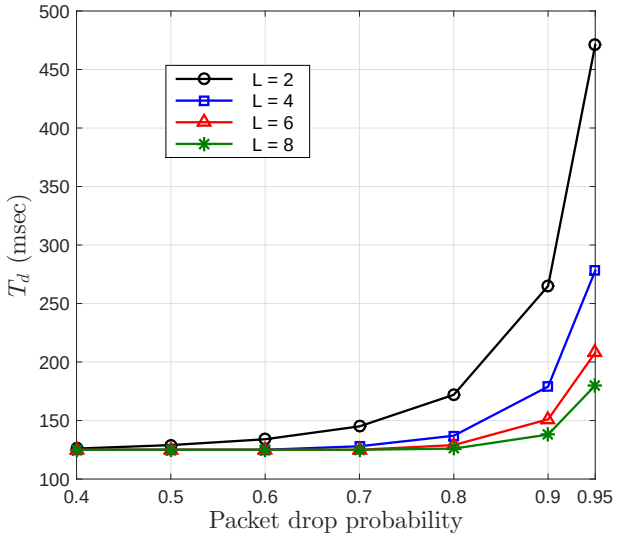

Fig. 9: The average detection time vs. packet dropout rate, $\Gamma_f = 0.1$ Hz, $\Gamma_A = 0.1$ pu, input SNR = 16 dB.

VI. Conclusion

In this paper, a robust and reliable structure for centralized detection of disturbances with noisy and intermittent synchrophasor data is proposed. It is verified that by employing

the interpolative PDC, severe packet dropout conditions can be compensated, resulting in a smaller average detection time. It is also shown that the proposed detection structure is robust against data noise at local PCCs. In the low and medium SNR regions, the performance of the central detection scheme remains superior in terms of probability of false detection. Moreover, this study reveals that how false detections can be further suppressed at the cost of higher detection time.

REFERENCES

[1] X. Fang, S. Misra, G. Xue, and D. Yang, "Smart grid - The new and improved power grid: A survey," *Commun. Surveys Tuts.*, vol. 14, no. 4, pp. 944-980, 2012.

[2] D. E. Olivares, et al., "Trends in microgrid control," *IEEE Trans. Smart Grid,* vol. 5, no. 4, pp. 1905-1919, Jul. 2014.

[3] X. Lu, et. al.,"Hierarchical control of parallel AC-DC converter interfaces for hybrid microgrids," *IEEE Trans. Smart Grid,*, vol. 5, no. 2, pp. 683 -692, Mar. 2014.

[4] Y. Mohamed, and A. A. Radwan, "Hierarchical control system for robust microgrid operation and seamless mode transfer in active distribution systems," *IEEE Trans. Smart Grid*, vol. 2, no. 2, pp. 352-362, Jun. 2011.

[5] H. Mahmood, and J. Jiang, "Modeling and control system design of a grid connected VSC considering the effect of the interface transformer type," *IEEE Trans. Smart Grid*, vol. 3, no. 1, pp. 122-134, Mar. 2012.

[6] *IEEE Standard for Synchrophasor Measurements for Power Systems*, Std C37.118.1-2011, Dec. 28, 2011.

[7] *IEEE standard for synchrophasor data transfer for power systems*, Std C37.118.2-2011, Dec. 28, 2011.

[8] E. O. Schweitzer, D. Whitehead, G. Zweigle, and K. G. Ravikumar, "Synchrophasor-based power system protection and control applications," *in Proc. 63rd Annu. Conf. Protective Relay Engineers*, 2010, pp. 1-10.

[9] J. D. L. Ree, V. Centeno, J. S. Thorp, and A. G. Phadke, "Synchronized phasor measurement applications in power systems," *IEEE Trans. Smart Grid,* vol. 1, no. 1, pp. 20-27, Apr. 2010.

[10] *IEEE guide for design, integration, and operation of distributed resource island systems with electric power systems*, Std 1547.4-2011, Jul. 20, 2011.

[11] S. I. Jang and K. H. Kim, "An islanding detection method for distributed generations using voltage unbalance and total harmonic distortion of current," *IEEE Trans. Power Del.*, vol. 19, no. 2, pp. 745-752, Apr. 2004.

[12] H. Laaksonen, "Advanced islanding detection functionality for future electricity distribution networks," *IEEE Trans. Power Del.,* vol. 28, no. 4, pp. 2056-2064, Oct. 2013.

[13] H. H. Zeineldin, "A Q-f droop curve for facilitating islanding detection of inverter-based distributed generation," *IEEE Trans. Power Electron.*, vol. 24, no. 3, pp. 665-673, Mar. 2009.

[14] S. Li, and X. Wang, "Monitoring disturbances in smart grids using distributed sequential change detection," *in Proc. 5th IEEE International Workshop on Computational Advances in Multi-Sensor Adaptive Processing (CAM SAP)*, 2013, pp. 432-435.

[15] A. Ukil, "Disturbance detection in the MV and the LV distribution networks using time-domain method," *in Proc. IEEE PES General Meeting*, 2014, pp. 1-5.

[16] E. Cotilla-Sanchez, P. D. H. Hines, and C. M. Danforth, "Predicting critical transitions from time series synchrophasor data," *IEEE Trans. Smart Grid,* vol. 3, no. 4, pp. 1832-1840, Sep. 2012.

[17] Y. Ge, et al., "Power system real-time event detection and associated data archival reduction based on synchrophasors," *IEEE Trans. Smart Grid,* vol. 6, no. 4, pp. 2088-2097, Jul. 2015.

[18] C.-i Chen, "A phasor estimator for synchronization between power grid and distributed generation system," *IEEE Trans. Ind. Electron.,* vol. 60, no. 8, pp. 3248-3255, May 2012.

[19] I. Kamwa, S. Samantaray, and G. Joos, "Compliance analysis of PMU algorithms and devices for wide-area stabilizing control of large power systems," *IEEE Trans. Power Syst.,* vol. 28, no.2, pp. 1766-1778, May 2013.

[20] M. Sumner, A. Abusorrah, D. Thomas, and P. Zanchetta, "Real time parameter estimation for power quality control and intelligent protection of grid-connected power electronic converters," *IEEE Trans. Smart Grid,* vol. 5, no. 4, pp. 1602-1607, Jul. 2014.

[21] Q. Shafiee, et al., "Robust networked control scheme for distributed secondary control of islanded microgrids," *IEEE Trans. Ind. Electron.*, vol. 61, no. 10, pp. 5363-5374, Oct. 2014.

[22] M. Karimi-Ghartemani and M. R. Iravani, "A nonlinear adaptive filter for on-line signal analysis in power systems: applications," *IEEE Trans. Power Delivery*, vol. 17, pp. 617-622, Apr. 2002.

[23] W. Zheng, H. Ma, X. He, "Modeling, analysis, and implementation of real time network controlled parallel multi-inverter systems," *in Proc.* 2012, International Power Electronics and Motion Control Conference (IPEMC), pp. 1125-1130.

[24] M. Karimi-Ghartemani, and H. Karimi, "Processing of symmetrical components in time-domain," *IEEE Trans. Power Syst.*, vol. 22, no. 2, pp. 572-579, May 2007.

[25] H. Karimi, A. Yazdani, and R. Iravani, "Negative-sequence current injection for fast islanding detection of a distributed resource unit," *IEEE Trans. Power Electron.*, vol. 23, no. 1, pp. 298-307, Jan. 2008.

[26] A. V. Oppenheim, R. W. Schafer, *Discrete-time signal processing*, Third edition, Prentice Hall, 2009.

[27] A. Papoulis, and S. U. Pillai, *Probability, Random Variables, and Stochastic Processes*, 4th Edition, McGraw-Hill, 2002.

[28] X. Songy, Z. Sahinogluz, and J. Guoz, "Transient disturbance detection for power systems with a general likelihood ratio test," *in Proc.* 2013, Acoustics, Speech and Signal Processing (ICASSP), IEEE International Conference on, pp. 2839-2843.

[29] T. Khalifa, et al., "Split- and aggregated-transmission control protocol (SA-TCP) for smart power grid," *IEEE Trans. Smart Grid,* vol. 5, no. 1, pp. 381-391, Jan. 2014.

[30] *IEEE guide for phasor data concentrator requirements for power system protection, control, and monitoring*, Std C37.244-2013, May. 10, 2013.

[31] K. D. Jones, A. Pal, and J. S. Thorp, "Methodology for performing synchrophasor data conditioning and validation," *IEEE Trans. Power Syst.*, vol. 30, no. 3, pp. 1121-1130, May 2015.

[32] J. Zhang, G. Welch, G. Bishop, and Z. Huang, "A two-stage Kalman filter approach for robust and real-time power system state estimation," *IEEE Trans. Sustain. Energy*, vol. 5, no. 2, pp. 629-636, Apr. 2014.

[33] J. T. Bialasiewicz, "Renewable energy systems with photovoltaic power generators: Operation and modeling," *IEEE Trans. Ind. Electron.*, vol. 55, no. 7, pp. 2752-2758, Jul. 2008.

Younes Seyedi (S'12) received the B.Sc. degree from University of Tehran, Tehran, Iran, in 2010, and the M.Sc. degree from Tehran Polytechnic, Tehran, Iran, in 2012, both in electrical engineering. He is currently pursuing his PhD program at Polytechnique Montreal, Montreal, QC, Canada. His current research interest is signal processing and data analysis for power grid monitoring, control, and protection. He is a graduate student member of IEEE.

Houshang Karimi (S'03-M'07-SM'12) received the B.Sc. and M.Sc. degrees from Isfahan University of Technology, Isfahan, Iran, in 1994 and 2000, respectively, and the Ph.D. degree from the University of Toronto, Toronto, ON, Canada, in 2007, all in electrical engineering. He was a Visiting Researcher and a postdoctoral Fellow in the Department of Electrical and Computer Engineering, University of Toronto, from 2001 to 2003 and from 2007 to 2008, respectively. He was with the Department of Electrical Engineering, Sharif University of Technology, Tehran, Iran, from 2009 to 2012. From June 2012 to January 2013, he was a Visiting Researcher in the ePower lab of the Department of Electrical and Computer Engineering, Queens University, Kingston, ON, Canada. He joined the Department of Electrical Engineering, Polytechnique Montreal, QC, Canada, in 2013, where he is currently an Assistant Professor. His research interests include control systems, distributed generations, and microgrid control.

Josep M. Guerrero (S'01-M'04-SM'08-FM'15) received the B.S. degree in telecommunications engineering, the M.S. degree in electronics engineering, and the Ph.D. degree in power electronics from the Technical University of Catalonia, Barcelona, in 1997, 2000 and 2003, respectively. Since 2011, he has been a Full Professor with the Department of Energy Technology, Aalborg University, Denmark, where he is responsible for the Microgrid Research Program. From 2012 he is a guest Professor at the Chinese Academy of Science and the Nanjing University of Aeronautics and Astronautics; from 2014 he is chair Professor in Shandong University; and from 2015 he is a distinguished guest Professor in Hunan University. His research interests is oriented to different microgrid aspects, including power electronics, distributed energy-storage systems, hierarchical and cooperative control, energy management systems, and optimization of microgrids and islanded minigrids; recently specially focused on maritime microgrids for electrical ships, vessels, ferries and seaports. Prof. Guerrero is an Associate Editor for the IEEE TRANSACTIONS ON POWER ELECTRONICS, the IEEE TRANSACTIONS ON INDUSTRIAL ELECTRONICS, and the IEEE Industrial Electronics Magazine, and an Editor for the IEEE TRANSACTIONS on SMART GRID and IEEE TRANSACTIONS on ENERGY CONVERSION. He has been Guest Editor of the IEEE TRANSACTIONS ON POWER ELECTRONICS Special Issues: Power Electronics for Wind Energy Conversion and Power Electronics for Microgrids; the IEEE TRANSACTIONS ON INDUSTRIAL ELECTRONICS Special Sections: Uninterruptible Power Supplies systems, Renewable Energy Systems, Distributed Generation and Microgrids, and Industrial Applications and Implementation Issues of the Kalman Filter; and the IEEE TRANSACTIONS on SMART GRID Special Issue on Smart DC Distribution Systems. He was the chair of the Renewable Energy Systems Technical Committee of the IEEE Industrial Electronics Society. He received the best paper award of the IEEE Transactions on Energy Conversion for the period 2014-2015. In 2014 and 2015 he was awarded by Thomson Reuters as Highly Cited Researcher, and in 2015 he was elevated as IEEE Fellow for his contributions on distributed power systems and microgrids.